Multifocal multiphoton microscopy

Jörg Bewersdorf, Rainer Pick, and Stefan W. Hell

High Resolution Optical Microscopy Group, Max-Planck-Institute for Biophysical Chemistry, D-37070 Göttingen, Germany

Received January 9, 1998

We present a real-time, direct-view multiphoton excitation fluorescence microscope that provides three-dimensional imaging at high resolution. Using a rotating microlens disk, we split the near-infrared light of a mode-locked titanium:sapphire laser into an array of beams that are transformed into an array of high-aperture foci at the object. We typically scan at 225 frames per second and image the fluorescence with a camera that reads out the images at video rate. For 1.4 aperture oil and 1.2 water immersion lenses at 780-nm excitation we obtained axial resolutions of 0.84 and 1.4 μm, respectively, which are similar to that of a single-beam two-photon microscope. Compared with the latter setup, our system represents a 40–100-fold increase in efficiency, or imaging speed. Moreover, it permits the observation with the eye of high-resolution two-photon images of (live) samples. © 1998 Optical Society of America

OCIS codes: 180.2520, 190.4180, 100.6890.

Nonlinear excitation through multiphoton absorption in the near-infrared (NIR) brings about a range of advantages in scanning fluorescence microscopy, such as inherent three-dimensional imaging without a confocal pinhole, reduced total photobleaching, and imaging of UV dyes with non-UV optical components as well as deeper penetration into scattering specimens.[1] These features and the reduced phototoxicity of NIR light demonstrate the unique potential of multiphoton microscopy (MPM) for three-dimensional imaging of live cells.

MPM is usually performed with a mode-locked Ti:sapphire (Ti:Sa) laser, providing a pulsed beam (~100-fs pulses at ~80 MHz) that is coupled into a beam-scanning microscope that scrutinizes the sample point by point. Serial scanning typically requires 0.5–2 s for a 50–200-μm squared image, which is insufficiently fast for a large number of applications. With some exceptions, the average power used at the sample, P_i, ranges from 3 to 10 mW because of saturation or other nonlinear effects that occur at higher power.[2] By emitting $P_{\mathrm{tot}} = 1$–2 W of power, that standard Ti:Sa laser offers abundant light for multiphoton excitation, so in fact 90–95% of the (expensive) laser light is discarded.

Real-time MPM by bilateral scanning with a line-shaped focus has been reported by Brakenhoff *et al.*[3] However, inefficient focusing of line scanning reduces the efficiency of multiphoton excitation and may call for higher pulse energy by regenerative amplification. Moreover, line scanning inevitably trades off axial resolution against speed. Whereas standard MPM routinely resolves fluorescent planes that are 1 μm apart, line-scanning systems fail for axial distances smaller than 3–6 μm.

In this Letter we demonstrate multifocal multiphoton microscopy (MMM), a simple yet powerful multiphoton method for providing real-time three-dimensional imaging with higher illumination efficiency and resolution. Figure 1 sketches the MMM arrangement. The expanded beam of a Ti:Sa laser illuminates an array of microlenses of 460-μm diameter and 6.0-mm focal length etched upon a rotating fused-silica disk. The lenses are arranged in a hexagonal pattern such that the illuminating beam is split into small beams, referred to as beamlets, and focused into an array of approximately 5×5 foci of ~6-μm beam waist at the prefocusing plane (PFP). The beamlets pass intermediate optics and are directed into a conventional Leica DM-IRB inverted fluorescence microscope. The role of the intermediate optics is to ensure that the array of foci is imaged into the focal plane of the lens and that each beamlet is parallel at, and overilluminates, the objective entrance pupil. The objective lens then produces a pattern of independent high-resolution foci at the sample, the number of which is determined by the magnification factor between the prefocusing plane and the focal plane of the objective lens. Typically we used a pattern of $5 \times 5 = 25$ foci, but one can easily vary the number by changing the intermediate optics.

The microlenses were manufactured (by S. Haselbeck, N. Lindlein, and J. Schwider, University of Erlangen, Germany) according to our specifications and are arranged with a constant helical pitch, forming spirals with 10 rows (Fig. 1). The center diameter of the

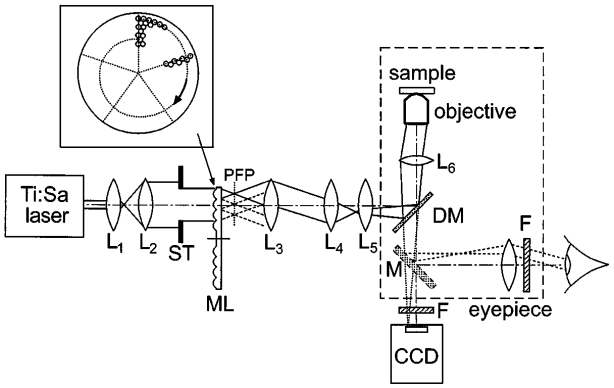

Fig. 1. Schematic of the MMM for real-time, direct-view nonlinear microscopy: L's, lenses; ML, microlens disk; M, optional mirror; F, short-pass filter; DM, dichroic mirror. Inset, the rotating microlens array.

0146-9592/98/090655-03$15.00/0

spiral is 80 mm. Rotating the disk by 360 deg renders three complete and independent scans of the focal plane. The disk is rotated at 75 Hz so that $3 \times 75 = 225$ scans/s are obtained. In fact, the disk was designed for 5 independent scans, totaling 375 scans/s. However, careful examination of the disk revealed slight variations of the focal length in 2 of the 5 independent scanning sections, so we restricted the operation to 225 scans/s by obstructing two sections. The image rate is ultimately determined by the camera frame rate, which is 32 and 67 images/s for 480×640 and 384×384 pixels, respectively, well within the video rate regime. Increasing the scan rate is technically straightforward, and its usefulness is limited only by the obtainable fluorescence photon flux.

Microlens arrays have been successfully used either as low-aperture objective lenses in reflection microscopy[4] or for increasing the illumination throughput in a pinhole Nipkow-disk confocal scanner.[5] In the latter case, stringent alignment to pinholes is required, which is reportedly challenging to achieve in practice. The MMM, however, dispenses with the pinhole disk, because three-dimensional imaging is accomplished by multiphoton absorption alone.

We optimize disk and intermediate optics for multiphoton excitation by ensuring the aforementioned beamlet power of $P_i = 3-10$ mW at the sample. After the inevitable losses in beam expansion and the optical train are taken into account, the optimal number of simultaneously used microlenses is of the order of $\Gamma = P_{\mathrm{tot}}/P_i \approx 20-50$. This number is in contrast to that for the Nipkow-disk system,[5] which uses 1000 lenses or more. For such a large number of microlenses the transient excitation intensity is reduced, severely compromising fast nonlinear excitation. Γ determines the gain in speed or in excitation efficiency with respect to its single-beam counterpart. In fact, the gain in speed can be estimated to be $2\,\Gamma \approx 40-100$ because the rotating disk does not involve scanning dead times, as is the case with standard galvanometric single-beam scanners.

The different foci are approximately 6.0 and 9.5 μm apart in the lateral direction for the oil and the water lenses, respectively, so they should not interfere with each other. Therefore an uncompromised axial resolution is expected. We measured the axial (z) response to an ultrathin lateral plane by scanning monomolecular films of polymerized dimethyl-*bis*(pentacosadiinoic-oxyethyl) ammonium bromide spread upon a cover slip.[6] The two-photon fluorescence z response for the plane is

$$I(z) = C \int_{-\infty}^{\infty} \int_{-\infty}^{\infty} h_{\mathrm{ill}}{}^2(x, y, z)\mathrm{d}x\mathrm{d}y\,,$$

whereby $h_{\mathrm{ill}}{}^2(x, y, z)$ denotes the squared illumination intensity in the focus. We measured $I(z)$ by scanning layers typically 20–40 μm in size for the 780-nm excitation wavelength. The curves are shown in Fig. 2. Whereas the bottoms of the curves are somewhat broader than expected in an ideal case, the FWHM's are equivalent to those of a standard single-beam two-photon microscope.[7] For the N.A. = 1.2 water immersion lens (Leica 63× W) the FWHM of the edge response is 1.40(5) μm. For the N.A. = 1.4 oil immersion lens (Leica 100× oil) we measured 0.84(5) μm.

Optical sectioning capability is further demonstrated in Fig. 3, which shows 12 xy sections through an autofluorescent pollen grain, 4 μm apart, imaged with the oil immersion lens and at 780-nm excitation. Each image, 384×384 pixels and $24\ \mu\mathrm{m} \times 24\ \mu\mathrm{m}$ in size, was recorded in 100 ms, totaling 1.2 s for the whole stack. Unlike for a single-beam MPM, we do not collect the light in a large area detector. Although we have not yet carried out direct comparisons, imaging with a camera is likely to be less suitable for penetrating strongly scattered samples. Nevertheless, the penetration depth of the MMM is expected to be considerably larger than that of confocal microscopy because of the reduced scattering of the NIR excitation light. In fact, xy image 11 of Fig. 3 is 40 μm deep in the scattering pollen grain. These results affirm the penetration capability of the camera-based MMM.

In general, we operated the MMM in the following power conditions: We reduced the initial ~1.4 W of the beam to ~630 mW by obstructing its outer part

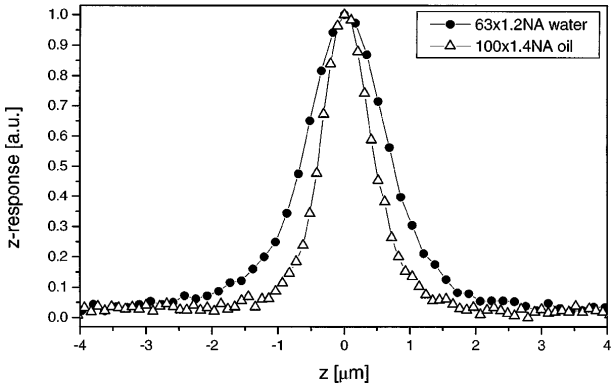

Fig. 2. Axial response to an ultrathin fluorescent plane, revealing the axial resolution of the MMM for high-N.A. water and oil immersion lenses.

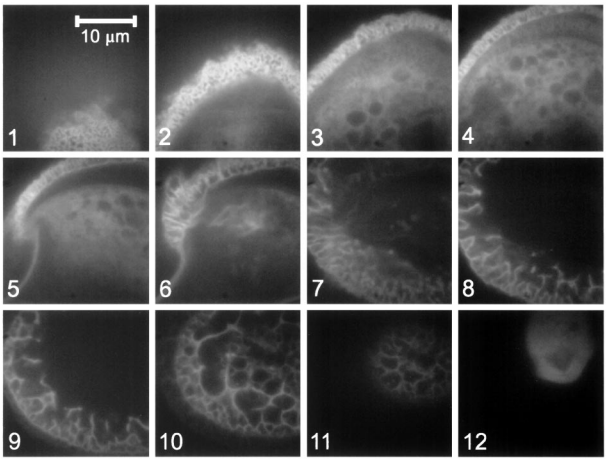

Fig. 3. Two-photon image stack of a pollen grain consisting of 12 xy layers at 4-μm axial distance. The imaging time for each layer was 100 ms; the stack was taken within 1.2 s. The pixel size is 62.5 nm × 62.5 nm; the data are not processed. Alternatively, the images can be viewed with the eye.

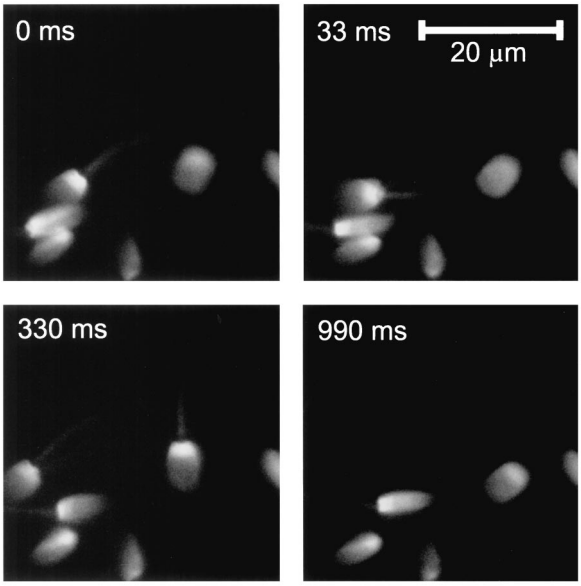

Fig. 4. xy images of live boar-sperm cells taken within 33 ms (30 images/s). Four typical images of a movie of 191 images are displayed. Note the movement of the sperm tail within the first 33 ms. The movie data are available on request.

and illuminating the microlenses with the center part of the original beam profile. Approximately 250 mW of power passed through the intermediate optics and reached the entrance pupil of the objective lens, so approximately 5–7 mW of power was obtained at each focus. The fluorescence light was separated by a long-pass dichroic mirror, and scattered excitation light was suppressed by 2 mm of colored glass (Schott, BG39). No residual laser light was observed.

One drawback of using the original beam profile is that the illumination of the image field is not necessarily flat. For the conditions shown in Fig. 3 the corners of the image are ~50% less intense than the center, as we established by imaging a uniform fluorescent plane. Potential remedies for this problem are linear scaling of the image brightness and expansion of the illumination beam (lenses L_1 and L_2 in Fig. 1). The light budget can be further enhanced by NIR antireflection coating of the optical train. Excitation efficiency can be increased tenfold by compression of the pulse width from the ~240 fs used here to the 10–20-fs regime by application of external group-velocity compensation. Both measures are useful for increasing the number of microlenses employed and therefore the image size. A simple and most promising approach, however, is to use dedicated beam-shaping optics to convert Gaussian beams into flat beams.

Note that the disk scanning mechanism does not imply dead times, as is the case with galvanometer scanners. The hexagonal arrangement of the microlenses ensures that 90% of the light hitting the array is converted into beamlets. In our experiments we did not suppress the remaining 10% from passing between the lenses. Not being prefocused by the microlenses, the residual light is defocused in the focal plane, and its effect is reduced by virtue of the nonlinear nature of the excitation. Nevertheless, the effect of the residual light is noticeable as a background when one is axially scanning through a thick fluorescence sea. We also attribute a part of the bottom of the z response (Fig. 2) to the residual unfocused light. However, simple technical measures (such as blackening the space between the microlenses) are expected to render uncompromised performance.

As a next step, we imaged live boar-sperm cells, the heads and tails of which we labeled with Hoechst 33342 and fluorescein, respectively. We recorded a stack of 191 images within 6-s monitoring of the movement of the live sperm cells in an aqueous medium. The images were recorded with the water immersion lens and read out every 33 ms. Figure 4 displays four xy images (384 × 384 pixels and 38 μm × 38 μm), the first two of which are just 33 ms apart.

Implementation of three-photon excitation[8,9] should be relatively simple. In addition, the MMM may prove useful for fast single-molecule imaging, especially when it is used with an intensified CCD. Instead of using a CCD camera it would also be possible to use the microlenses in conjunction with photomultiplier arrays, in which case the optics and the scanning mechanism would require a different design. However, the MMM described here outperforms standard two-photon approaches in terms of speed, sensitivity, and simplicity. The rotating disk and a large part of the intermediate optics are outside the body of the Leica inverted microscope, so in fact any commercial fluorescence microscope could be converted into a MMM. Moreover, by simply blocking the NIR excitation light in the eyepiece with an absorption filter we used the MMM to achieve real-time observation of two-photon images with the eye. Whereas it was not possible to view, for example, the interior of a pollen grain by conventional arc lamp illumination, the view provided by the MMM was of stunning clarity.

Address any correspondence to S. W. Hell at shell@gwdg.de; fax: +49 551 201 1085.

References

1. W. Denk, J. H. Strickler, and W. W. Webb, Science **248,** 73 (1990).
2. K. König, P. C. T. So, W. W. Mantulin, B. J. Tromberg, and E. Gratton, J. Microsc. **183,** 197 (1996).
3. G. J. Brakenhoff, J. Squier, T. Norris, A. C. Bliton, M. H. Wade, and B. Athey, J. Microsc. **181,** 253 (1996).
4. H. J. Tiziani, R. Achi, R. N. Krämer, and L. Wiegers, Appl. Opt. **35,** 120 (1996).
5. A. Ichihara, T. Tanaami, K. Isozaki, Y. Sugiyama, Y. Kosugi, K. Mikuriya, M. Abe, and I. Uemura, Bioimages **4,** 52 (1996).
6. M. Schrader, U. G. Hofmann, and S. W. Hell, "Ultrathin fluorescent layers for monitoring the axial resolution in confocal and two-photon fluorescence microscopy," J. Microsc. (to be published).
7. S. W. Hell, P. E. Hänninen, A. Kuusisto, M. Schrader, and E. Soini, Opt. Commun. **117,** 20 (1995).
8. S. W. Hell, K. Bahlmann, M. Schrader, A. Soini, H. Malak, I. Gryczynski, and J. R. Lakowicz, J. Biomed. Opt. **1,** 71 (1996).
9. D. L. Wokosin, V. E. Centonze, S. Crittenden, and J. White, Bioimaging **4,** 208 (1996).